Developmental Biology 337 (2010) 220–232

Contents lists available at ScienceDirect

Developmental Biology

journal homepage: www.elsevier.com/developmentalbiology

Nanos functions to maintain the fate of the small micromere lineage in the sea urchin embryo

Celina E. Juliano, Mamiko Yajima, Gary M. Wessel *

Department of Molecular and Cell Biology and Biochemistry, Brown University, 185 Meeting St., Providence, RI 02912, USA

ARTICLE INFO

Article history:
Received for publication 4 September 2009
Revised 9 October 2009
Accepted 21 October 2009
Available online 28 October 2009

Keywords:
Nanos
Vasa
Sea urchin
Small micromeres
Germline
Primordial germ cell
Multipotent
Piwi

ABSTRACT

The translational regulator *nanos* is required for the survival and maintenance of primordial germ cells during embryogenesis. Three *nanos* homologs are present in the genome of the sea urchin *Strongylocentrotus purpuratus*, all of which are expressed with different timing in the small micromere lineage. This lineage is set-aside during embryogenesis and contributes to constructing the adult rudiment. Small micromeres lacking *Sp-nanos1* and *Sp-nanos2* undergo an extra division and are not incorporated into the coelomic pouches. Further, these cells do not accumulate Vasa protein even though they retain *vasa* mRNA. Larvae that develop from *Sp-nanos1* and *2* knockdown embryos initially appear normal, but do not develop adult rudiments; although they are capable of eating, over time they fail to grow and eventually die. We conclude that the acquisition and maintenance of multipotency in the small micromere lineage requires *nanos*, which may function in part by repressing the cell cycle and regulating other multipotency factors such as *vasa*. This work, in combination with other recent results in *Ilyanassa* and *Platynereis dumerilii*, suggests the presence of a conserved molecular program underlying both primordial germ cell and multipotent cell specification and maintenance.

Introduction

Multicellular animals are composed of many specialized cell types, but only the germ cells are capable of passing genetic information on to the next generation. To propagate the species, select cells are set aside during embryogenesis to form the future germline. A conserved set of genes is required to specify and/or maintain the germline during embryogenesis. *Nanos*, one such gene, is required for fertility in *Drosophila*, *Caenorhabditis elegans*, zebrafish, and mice (Kobayashi et al., 1996; Subramaniam and Seydoux, 1999; Koprunner et al., 2001; Tsuda et al., 2003). Germline progenitor cells of the *Drosophila* embryo (pole cells) that lack *nanos* exhibit various defects, including an inability to migrate to the gonad, loss of transcriptional and mitotic quiescence, expression of somatic cell markers, and apoptosis; consequently *nanos*-null pole cells fail to develop into functional germ cells (Kobayashi et al., 1996; Asaoka-Taguchi et al., 1999; Deshpande et al., 1999; Hayashi et al., 2004). *Nanos* functions together with *pumilio* to repress the translation of the cell cycle regulator *cyclin B* and the pro-apoptotic gene *head involution defect* (*hid*) in pole cells, thus directly controlling the cell cycle and survival of these cells (Asaoka-Taguchi et al., 1999; Kadyrova et al., 2007). Similarly, loss of *nanos* function in *C. elegans* leads to premature primordial germ cell (PGC) proliferation and in mice its loss results in PGC apoptosis. Thus, *nanos* appears to have conserved functions in animal germlines (Subramaniam and Seydoux, 1999; Suzuki et al., 2008).

In addition to its germline functions, *nanos* is expressed more broadly in multipotent cells. In *Hydra* polyps *nanos* is expressed in multipotent interstitial cells (I-cells), which give rise both to several somatic cell types and to germ cells (Mochizuki et al., 2000). In the polychaete annelid, *Platynereis dumerilii*, and the snail, *Ilyanassa*, both of which develop through a larval stage, multipotent cells of the embryo specifically express *nanos* (Rebscher et al., 2007; Rabinowitz et al., 2008). The *nanos*-positive multipotent cells of *P. dumerilii* give rise to both all of the trunk mesodermal cell types of the adult segments, and to germ cells (Rebscher et al., 2007). *Nanos* is also expressed in the 4d lineage of *Ilyanassa*; this lineage gives rise to adult mesodermal and endodermal tissues (Render, 1997; Rabinowitz et al., 2008). Functional studies in *Ilyanassa* suggest that *nanos* is critical to maintain the fate of the 4d lineage, as the loss of *nanos* function in embryos results in the loss of all 4d-derived adult structures (Rabinowitz et al., 2008).

The majority of the species in the phylum Echinodermata are maximal indirect developers in which embryogenesis culminates with the formation of a free-swimming, feeding larva that supports its developing adult rudiment. At metamorphosis the rudiment will give rise to the juvenile. During embryogenesis in these maximally indirect developing organisms, groups of cells are set aside for use in adult rudiment construction. Unlike the cells that will give rise to the larval structures *per se*, these cells retain proliferative and developmental potential (Peterson et al., 1997). The small micromere lineage of the sea

* Corresponding author.
E-mail address: rhet@brown.edu (G.M. Wessel).

0012-1606/$ – see front matter © 2009 Elsevier Inc. All rights reserved.
doi:10.1016/j.ydbio.2009.10.030

urchin embryo, which specifically accumulates *nanos* mRNA, is one such group of set-aside cells (Juliano et al., 2006). During embryogenesis, four small micromeres are formed at the 32-cell stage as a result of two unequal cleavage divisions: a vegetal unequal fourth cleavage division gives rise to a 16-cell embryo with 4 micromeres and a subsequent unequal division of the micromeres results in the formation of 4 small micromeres. In the blastula the small micromeres reside at the vegetal plate where they divide once before being transported through the blastocoel at the tip of the archenteron during gastrulation. The eight small micromere descendants are then partitioned into the left and right coelomic pouches, the site of adult rudiment formation in the pluteus larva. The coelomic pouches are derived from two sources: 60% from a subset of the macromere descendants and 40% from the small micromere descendants (Cameron et al., 1991). During larval formation, the small micromere descendants move into the coelomic pouches from their position at the tip of the archenteron in the gastrula (Pehrson and Cohen, 1986; Tanaka and Dan, 1990). It is clear that the small micromere lineage gives rise solely to adult tissues, but the identity of these tissues has not been experimentally determined (Pehrson and Cohen, 1986; Tanaka and Dan, 1990).

Due to both their slow cell cycle and contribution to adult tissues, it has been suggested that the small micromeres are germline precursors (Tanaka and Dan, 1990). In support of this hypothesis, the conserved germline genes *nanos*, *vasa*, and *piwi* are specifically expressed in the small micromeres (Juliano et al., 2006; Voronina et al., 2008). However, the small micromeres proliferate shortly after they reach the coelomic pouches (Tanaka and Dan, 1990). This would not be expected if the small micromeres were indeed equivalent to PGCs, which typically stay mitotically and/or transcriptionally quiescent until they reach the somatic gonad (Su et al., 1998; Subramaniam and Seydoux, 1999; Seydoux and Braun, 2006; Seki et al., 2007). An alternative hypothesis suggests that the small micromeres are instead multipotent and will give rise to various adult tissues (Ransick et al., 1996). These seemingly contradictory hypotheses can be reconciled when considering recent results pointing to a broader role for conserved germline genes in multipotent cells that give rise to both germ cells and to somatic cells (Mochizuki et al., 2000; Mochizuki et al., 2001; Reddien et al., 2005; Rebscher et al., 2007; Palakodeti et al., 2008; Pfister et al., 2008; Rabinowitz et al., 2008; Swartz et al., 2008). Thus, the small micromere lineage may give rise to both germ and somatic cell types of the sea urchin adult. Here we test the function of *nanos* in the small micromere lineage, a likely multipotent cell population, in order to further understand the potentially ancestral role of this gene in establishing and maintaining multipotential cell populations during embryogenesis.

Materials and methods

Animals

Strongylocentrotus purpuratus were housed in aquaria with artificial seawater (ASW) at 16 °C (Coral Life Scientific Grade Marine Salt; Carson, CA). Gametes were acquired by either 0.5M KCl injection or by shaking. Eggs were collected in ASW or filtered seawater and sperm was collected dry. To obtain embryos, fertilized eggs were cultured in ASW or filtered seawater at 16 °C. When early stage embryos were required for labeling, fertilization was performed in the presence of 1 mM 3-amino-triazol (3-AT) (Sigma; St. Louis, MO) to inhibit cross-linking of the fertilization envelopes. Before fixing, envelopes were removed by passing the embryos through 80 μM and 64 μM Nitex® mesh. Careful monitoring was required to ensure the integrity of the embryos.

Identification and cloning of Sp-nanos homologs

Three *Sp-nanos* homologs were identified in the *S. purpuratus* genome (spbase.org) by BLAST analysis (Altschul et al., 1990). Full-length genes (complete ORF plus some UTR sequences) were amplified from 24- or 48-h embryonic cDNA by PCR and cloned into pGEMT-EZ (Promega; Madison, WI) for sequencing. Amplification of *Sp-nanos2* required only one round of PCR (Juliano et al., 2006), whereas *Sp-nanos1* and *Sp-nanos3* required 2 rounds of PCR with nested primer sets to amplify full-length sequences. Primers were as follows (listed 5′ to 3′): Sp-Nanos2-F1—TTCTTGACTAGCTCTACGACGTACT; Sp-Nanos2-R1—TCGAGACGAGTAGACCCTACA; Sp-Nanos1-F1 – TAGATCATTCAAGACAAGCTCT; Sp-Nanos1-F2—GGAAGTACATCGCATTTTACAA; Sp-Nanos1-R1—CTAGAAGATCTTAACGGTCG; Sp-Nanos1-R2—TGGGGTTCGATACTGGGATC; Sp-nanos3-F1—GTACACCCGTGTCCGTGAG; Sp-nanos3-F2—CCAATACAACATTAATCTTCAAG; Sp-nanos3-R1—TGTCAAAAACTTTGTGCCAGAA; Sp-nanos3-R2—TACTTCCTACATAGGACGAC. The 3′ and 5′ UTR sequences of the *Sp-nanos* homologs were extended with RACE (Ambion; Austin, TX). Using PAUP, an unrooted neighbor-joining phylogram was made from full-length *nanos* coding sequences collected from NCBI (for accession numbers see Fig. 1); bootstrap replicate values are from 1000 iterations (Swofford, 2002).

Whole mount RNA in situ hybridization (WMISH)

Sequences used to make antisense WMISH probes for *Sp-nanos1*, *Sp-nanos2*, and *Sp-nanos3* were amplified from 48-h embryonic cDNA and cloned into pGEMT-EZ. The *Sp-nanos3* probe template includes the entire ORF plus 650 bases of the 3′UTR; the primer sets used for nested PCR are described above. Two *Sp-nanos2* probes were used: the first is previously described in Juliano et al. (2006) and the second includes 950 bases of the 3′UTR. The primer set used to amplify the *Sp-nanos2* 3′UTR is as follows (listed 5′ to 3′): Sp-Nanos2-F2—TGTAGGGTCTACTCGTCTCGA; Sp-Nanos2-R2—CACCCAGCAATCAGTACTTTC. The *Sp-nanos1* probe template includes the entire ORF plus 130 bases of the 3′UTR; the nested primer sets used for amplification are as follows: forward primers are described above; Sp-nanos1-R3—AGAATGGAGTACTTGCGTAC; Sp-nanos1-R4—ATACACCCAGCAATCAGTAC. The pGEMT-EZ plasmids were linearized using either *Sal*I (T7 transcription) or *Nco*I (SP6 transcription) (Promega; Madison, WI). Antisense DIG-labeled RNA probes were constructed using a DIG RNA labeling kit (Roche; Indianapolis, IN). WMISH experiments were performed as previously described (Minokawa et al., 2004) and the alkaline phosphatase reaction was carried out for 22 h. The *Sp-vasa* probe is described in Juliano et al., 2006. A non-specific DIG-labeled RNA probe complimentary to pSPT 18 (Roche; Indianapolis, IN) was used as a negative control. For uninjected embryos, all steps were carried out in 2 mL screw-top tubes (National Scientific Supply; Claremont, CA). For injected and manipulated embryos, all steps were carried out in 96-well round-bottom PVC plates (ThermoFisher Scientific; Rockford, IL). Samples were imaged on a Zeiss Axiovert 200M microscope equipped with a Zeiss color AxioCam MRc5 camera (Carl Zeiss, Inc.; Thornwood, NY).

Fluorescent RNA in situ hybridization (FISH)

Sp-vasa FISH on mock-injected and *Sp-nanos1* and *2* knockdown embryos was performed as previously described above through the blocking steps. Subsequently, samples were incubated overnight with anti-DIG-POD (Roche; Indianapolis, IN) diluted 1:1500 in blocking buffer II (Minokawa et al., 2004) at room temperature with rotation. Samples were washed 6 times for 1 h in TBST (10 mM Tris-HCl, pH7.4; 0.15M NaCl; 0.1% Tween-20). Signal was detected using the Tyramide Signal Amplification (TSA) kit (Perkin Elmer; Waltham, MA). Samples were washed once with 1X amplification solution and then incubated with cyanine 3 TSA working solution for 15 min. Samples were washed 6 times with TBST, the 5th wash contained a 1:1000 dilution of a 10 mg/mL Hoechst stock solution (Molecular Probes; Carlsbad, CA) for DNA labeling. Z-stacks were acquired for 5 mock-injected and

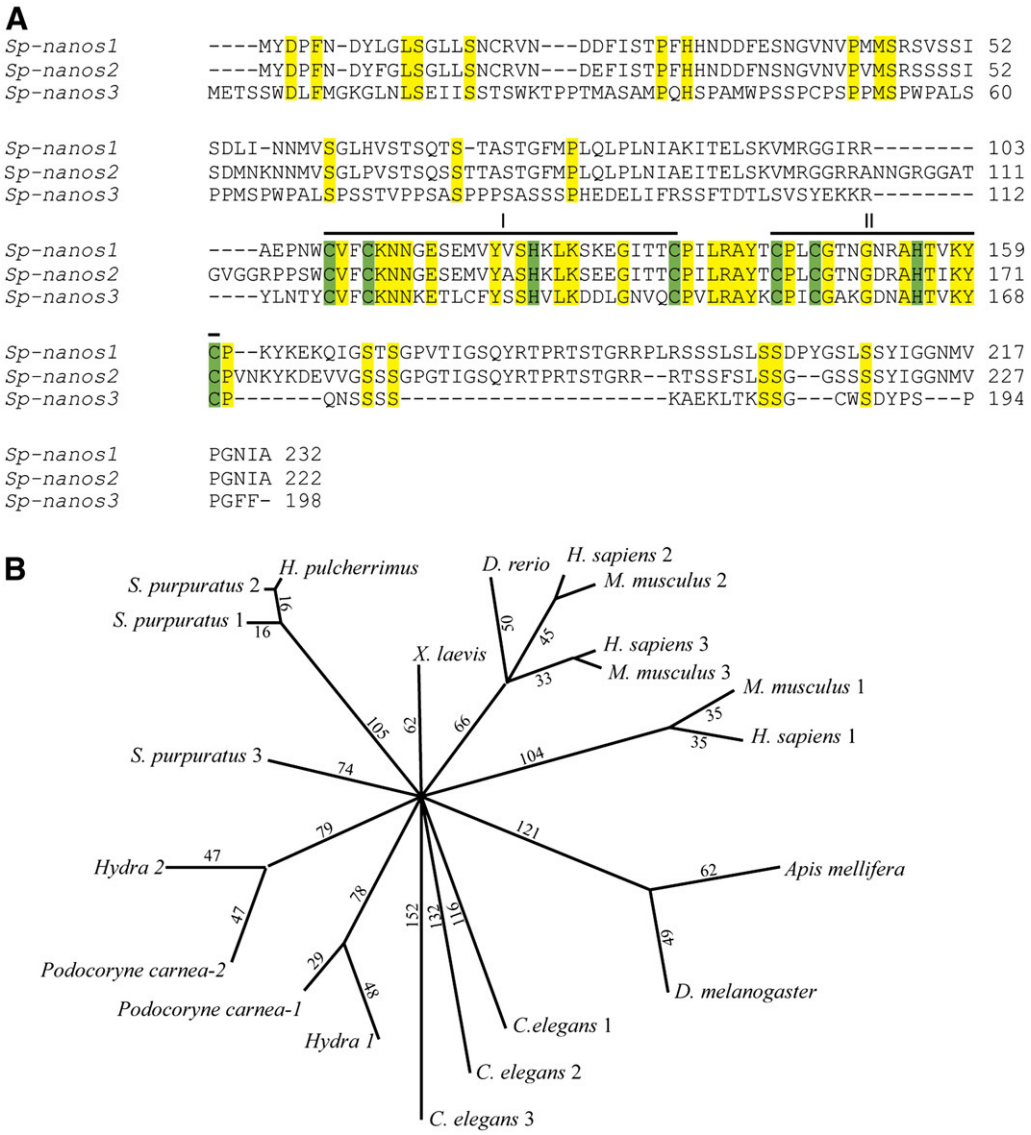

Fig. 1. Three *nanos* homologs are present in the *S. purpuratus* genome: *Sp-nanos1*, *Sp-nanos2*, and *Sp-nanos3*. (A) A sequence alignment of the three *S. purpuratus nanos* homologs reveals two conserved CCHC zinc finger motifs common to all *nanos* homologs. The amino acid sequences of *Sp-nanos1* and *Sp-nanos2* are nearly identical, except *Sp-nanos2* contains an additional 12 amino acids just before the first zinc finger (104–115). Conserved amino acids are highlighted in yellow, and the CCHC zinc finger amino acids are highlighted in green. (B) An unrooted neighbor-joining phylogram demonstrates that the three *Sp-nanos1* and *Sp-nanos2* are more closely related to each other than *Sp-nanos3*. Numbers indicate bootstrap replicate values from 1000 iterations. NCBI accession numbers are as follows: *H. sapiens-1* (Q8WY41), *H. sapiens-2*: (P60321), *H. sapiens-3* (P60323), *M. musculus-1* (Q80WY3), *M. musculus-2* (P60322), *M. musculus-3* (P60324), *X. laevis* (I51603), *D. rerio* (AAH97090), *D. melanogaster* (P25724), *C. elegans-1* (NP_496358), *C. elegans-2* (NP_495452), *C. elegans-3* (T27135), *Apis mellifera* (ABC41342), *Hemicentrotus pulcherrimus* (BAE53723), *Musca domestica* (AAA87461), *Nematostella vectensis-1* (AAY67907), *Nematostella vectensis-2* (AAY67908), *Podocoryne carnea-1* (AAU11513), *Podocoryne carnea-2* (AAU11514), *Hydra magnipapillata-1* (BAB01491), *Hydra magnipapillata-2* (BAB01492).

14 *Sp-nanos1/2* MASO-injected embryos on an LSM 510 laser scanning confocal microscope (Carl Zeiss, Inc.; Thornwood, NY) and *Sp-vasa*-positive cells were counted.

Real-time quantitative PCR (QPCR)

RNA was extracted from 75 mock-injected and 75 *Sp-nanos1/2* MASO-injected embryos at each time point (1 day, 3 days, 5 days, 7 days) using the RNeasy Micro Kit (Qiagen; Valencia, CA). cDNA was prepared using the TaqMan ® Reverse Transcription Reagents kit (Applied Biosystems; Foster City, CA). QPCR was performed on the 7300 Real-Time PCR system (Applied Biosystems; Foster City, CA) with the SYBER Green PCR Master Mix Kit (Applied Biosystems; Foster City, CA). *Sp-nanos1* and *2* and *Sp-vasa* primer sets are described in Juliano et al. (2006). Experiments were run in triplicate and the data were normalized to ubiquitin RNA levels.

Sp-nanos2 antibody generation and immunoblot analysis

Full-length *Sp-nanos2* was cloned downstream of the 6× Histidine tag found in the pTAT vector (Nagahara et al., 1998). Recombinant protein was expressed in BL21 bacteria, purified on a ProBond nickel column (Invitrogen; Carlsbad, CA), and used to raise antiserum in rabbits as previously described (Wong and Wessel, 2004). For affinity purification, recombinant Sp-Nanos2 protein was immobilized using the Pierce AminoLink Plus Immobilization Kit (ThermoFisher Scientific; Rockford, IL) as per the manufacturer's instructions. Heat-inactivated antiserum was passed over the antigen-immobilized column and bound antibodies were eluted with 1 mL 100 mM glycine (pH 2.5) into 50 µL 1 M Tris (pH 9.5).

For immunoblot analysis of Sp-Nanos2, *S. purpuratus* uninjected and *Sp-nanos1/2* MASO-injected embryos were cultured to the gastrula stage and were used to make embryo extracts as follows.

Two hundred embryos were pelleted, resuspended in heated SDS sample loading buffer, boiled for 5 min, and DTT (Roche; Indianapolis, IN) was added at a final concentration of 5 mM. Samples were incubated at 100 °C for 5 min, spun at 14K RPM for 2 min, then loaded onto Tris-glycine, 4–20% gradient gels (Invitrogen; Carlsbad, CA). After transfer to nitrocellulose (Pall Corporation; Pensacola, FL), blots were probed with affinity-purified *Sp-nanos2* antibody at 1 μg/mL in Blotto (3% dry milk, 170 mM NaCl, 50 mM Tris, 0.05% Tween20). For visualization, blots were probed with an anti-rabbit-HRP secondary antibody diluted 1:5000 in Blotto (Jackson ImmunoResearch Laboratories; West Grove, PA), and visualized by standard ECL detection. Blots were stripped by two 30-min incubations at 80 °C in 200 mM glycine-HCl, 0.05% Tween20 (pH 2.5) and then re-probed with α-YP30 serum diluted 1:30,000 in Blotto (Wessel et al., 2000).

Immunofluorescence

Embryos were cultured as described above and samples were collected at indicated stages of development for whole mount antibody labeling. Embryos were fixed in 4% paraformaldehyde (Electron Microscopy Sciences; Hatfield, PA)/ASW for 10 min at room temperature, extracted in 100% MeOH (−20 °C) for 1 min, washed 3 times with PBS-Tween, and stored at 4 °C. Antibody labeling was preceded by a blocking step of at least 30 min in 4% sheep serum (Sigma; St. Louis, MO) /PBS-Tween. For labeling, embryos were incubated overnight at 4 °C with affinity-purified *Sp-nanos2* antibody diluted in blocking buffer to a concentration of 10 μg/mL. The embryos were washed 3 times with PBS-Tween and then incubated with anti-rabbit Cy3 conjugated antibody (Jackson ImmunoResearch; West Grove, PA) diluted 1:300 in blocking buffer for 1 h at room temperature. The embryos were then washed 3 times with PBS-Tween. Labeled embryos were imaged on a Zeiss AxioPlan microscope (Carl Zeiss Inc.; Thornwood, NY) with an Orca-ER CCD camera (Hammamatsu Corporation; Bridgewater, NJ). For injected and manipulated samples the immunolabeling procedure was the same with the following exceptions: Samples were fixed in 24-well BSA-coated polystyrene plates (Corning; Corning, NY) or 9-well glass plates. Advanced larvae were fixed with 90% MeOH for 1 h at −20 °C. All subsequent labeling steps were done in BSA-coated 60-well mini trays (Nunc; Rochester, NY). For Sp-Vasa immunolabeling, *Sp-vasa* antibody was diluted in blocking buffer to a concentration of 10 μg/mL (Voronina et al., 2008). The secondary antibody used was anti-rabbit Alexa Flour® 488 conjugated antibody (Invitrogen; Carlsbad, CA) diluted 1:500 in blocking buffer. Embryos and larvae were incubated with 1:1000 dilution of a 10 mg/mL Hoechst stock solution for 10 min in PBS-Tween for DNA labeling (Molecular Probes; Carlsbad, CA). Labeled embryos and larvae were imaged on an LSM 510 laser scanning confocal microscope (Carl Zeiss, Inc.; Thornwood, NY).

Microinjections

Morpholino antisense oligos (MASO) directed against the *Sp-nanos1* and/or *Sp-nanos2* 5′UTR were synthesized by Gene Tools (Philomath, OR). Microinjections of zygotes were performed as previously described (Cheers and Ettensohn, 2004). In brief, eggs were de-jellied with acidic sea water (pH 5.0), washed with ASW or filtered sea water three times, rowed with a mouth pipette onto protamine sulfate-coated 60×15 mm petri dishes, fertilized in the presence of 1 mM 3-AT, and injected using the Femto Jet ® injection system (Eppendorf; Hamburg, Germany). To make the injection needles, 1×90 mm glass capillaries with filaments (Narishige; Tokyo, Japan) were pulled on a vertical needle puller (Narishige; Tokyo, Japan). Morpholino injection solutions were made as follows: 500 μM MASO, 20% glycerol, 1 mM 10,000 MW Dextran conjugated to Texas Red ® (Invitrogen; Carlsbad, CA). For rescue experiments, *Sp-nanos1* mRNA with *Xenopus* β-globin UTRs was added to the morpholino injection solution to a final concentration of approximately 500 ng/μL. *Sp-nanos1* mRNA was made using an SP6 Message Machine kit as per the manufacture's instructions (Ambion; Austin, TX). Mock injection solutions were identical, but without morpholino or RNA. Injected embryos were removed from the injection plate by mouth pipette and cultured at 16 °C in noble agar-coated 24-well plates for up to 3 days. If larval stages were required, embryos were moved to pre-rinsed 15 or 50 mL conical tubes (BD Falcon; Franklin Lakes, NJ) and rotated end over end at 16 °C. Larvae were washed and fed every 3–4 days with the algal species *Chaetoceros gracilis* (UTEX; Austin, TX). To induce metamorphosis, between 6 and 8 weeks after fertilization, larvae were moved to 60×15 mm petri dishes with biofilm and incubated at 16 °C.

Micromere transplants

Zygotes were injected, as described above, with either *Sp-nanos1/2* MASO or mock injection solutions. Both injected (donor) and uninjected (recipient) embryos were moved by mouth pipette from the injection plate to BSA-coated 60×15 mm petri dishes. The process of removing the embryos from the injection plate removes the fertilization envelope. Embryos were cultured to the 16-cell stage and then micromere transplants were performed as previously described (Yajima, 2007). However, instead of rhodamine, donor micromeres were labeled with Texas Red ® conjugated to dextran from the injection solution. After incorporation of the donor micromeres into the recipient embryo, transplanted embryos were moved to single wells of a polystyrene 96-well plate (Corning; Corning, NY) and cultured at 16 °C. After 3 days, transplanted embryos were moved to individual 15 mL conical tubes and cultured to late larval stages as described above. Images of transplanted embryos and larvae were taken on a Zeiss AxioPlan microscope (Carl Zeiss Inc.; Thornwood, NY) with an Orca-ER CCD camera (Hammamatsu Corporation; Bridgewater, NJ).

Results

Three nanos homologs are expressed in the small micromere lineage

A computational search, using basic local alignment search tool (BLAST), of the *S. purpuratus* genome (spbase.org) revealed the presence of 3 *nanos* homologs (Altschul et al., 1990), which were designated as *Sp-nanos1*, *Sp-nanos2*, and *Sp-nanos3* (Fig. 1A; Juliano et al., 2006). The open reading frames (ORFs) of *Sp-nanos1* and *Sp-nanos2* have approximately 90% identical nucleotide sequences and nearly identical amino acid sequences. The most significant difference between the ORFs of *Sp-nanos1* and *Sp-nanos2* is an additional 12 amino acids (104–115) present in *Sp-nanos2* (Fig. 1A). However, *Sp-nanos1* and *Sp-nanos2* have different flanking sequences in the genome and thus appear to be two distinct genes rather than different alleles of the same gene. Furthermore, 3′ RACE analysis demonstrates that the *Sp-nanos2* 3′UTR is approximately 1.2 kb. The *Sp-nanos1* 3′ UTR is only 0.2Kb long and shares 60% sequence identity with the first 0.2 kb of the *Sp-nanos2* 3′ UTR (data not shown). By contrast, *Sp-nanos3* shares approximately 20% amino acid sequence identity over the entire ORF with *Sp-nanos1* and *Sp-nanos2* (Fig. 1A). A phylogenetic analysis demonstrates that the three *S. purpuratus nanos* homologs cluster together on an unrooted neighbor joining tree, suggesting that they arose from recent duplication events (Fig. 1B).

Previously published whole-mount RNA *in situ* hybridization (WMISH) results revealed that *Sp-nanos2* is expressed in the small micromere lineage of the *S. purpuratus* embryo (Juliano et al., 2006). Here we demonstrate that *Sp-nanos2* is first detected in the small micromeres at the 60-cell stage (Fig. 2C). Probes directed against the *Sp-nanos1* ORF and the *Sp-nanos2* 3′UTR also indicate that these

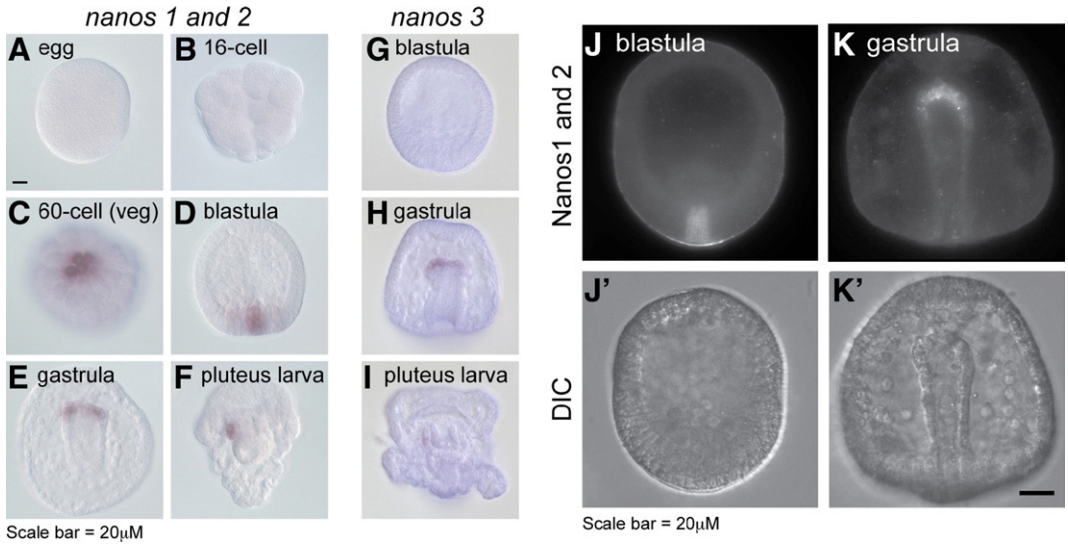

Fig. 2. *Nanos* mRNA and protein accumulates in the small micromeres. (A–I) *Sp-nanos1/2* and *Sp-nanos3* whole-mount RNA *in situ* hybridization (WMISH) was performed on the indicated *S. purpuratus* embryonic stages. *Sp-nanos1* and *Sp-nanos2* share approximately 90% identity at the nucleotide level, thus WMISH probes likely cross-react. (A–F) *Sp-nanos1* and *2* is first detected in the small micromeres at the 60-cell stage and remains associated with this lineage in the blastula, gastrula, and the left coelomic pouch of the early pluteus. (G–I) *Sp-nanos3* is first detected in the small micromere lineage at the tip of the archenteron in the gastrula, and then in the left coelomic pouch of the early pluteus. (J, K) Immunofluorescence analysis demonstrates that Sp-Nanos1 and 2 protein accumulates specifically in the small micromere lineage in the (J, J') blastula and (K, K') gastrula.

transcripts accumulate in the small micromere lineage (Supp. Figure 1). However, it is not possible to make a specific *Sp-nanos1* probe due to its short 3′UTR, and it is likely that WMISH probes directed against the ORFs of these two homologs significantly cross-hybridize. *Sp-nanos3* transcripts accumulate specifically in the small micromere lineage of the gastrula and then are associated with the left coelomic pouch of the pluteus (Figs. 2G–I). We conclude that all three *Sp-nanos* homologs are dynamically and specifically expressed in the small micromere lineage.

A polyclonal antibody generated against the entire Sp-Nanos2 ORF recognizes an approximately 24 kDa band on an immunoblot, consistent with the 24.7 kDa predicted molecular weight (MW) of *Sp-nanos2* (Fig. 3E and data not shown). The specificity of the antibody was tested by pre-incubation of the antibody with recombinant Sp-Nanos2 protein and reactivity was lost on an immunoblot when it was pre-incubated with recombinant Sp-Nanos2, thus confirming the specificity of the antibody (data not shown). However, given the nearly identical amino acid sequences of Sp-nanos1 and Sp-nanos2, this antibody likely recognizes both proteins. Since the predicted MW of Sp-Nanos1 (24.2 kDa) is only 500 Da less than Sp-Nanos2, we are not able to resolve these two homologs using SDS-PAGE. Immunofluorescence analysis demonstrates that Sp-Nanos1 and 2 proteins accumulate specifically in the small micromere lineage, similar to the *Sp-nanos1* and *2* transcripts (Figs. 2J, K).

Sp-nanos1 and Sp-nanos2 are required for accumulation of Sp-Vasa protein

To determine the function of *Sp-nanos1* and *Sp-nanos2* homologs during sea urchin embryogenesis, we employed an antisense morpho-

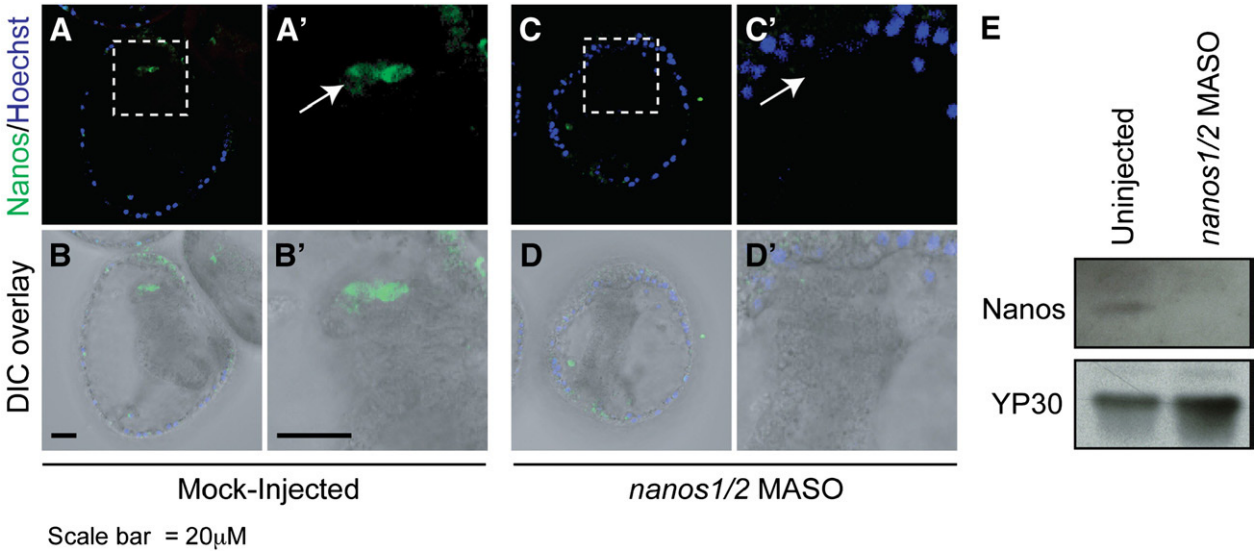

Fig. 3. A morpholino targeted against both *Sp-nanos1* and *Sp-nanos2* reduces Sp-Nanos1 and 2 protein expression. (A, B) Sp-Nanos1 and 2 protein (green) is detected in the small micromere lineage at the tip of the archenteron (arrow) in the gastrula of mock-injected embryos, (C, D) but is not detected in embryos injected with a morpholino that targets the 5′ UTR of both *Sp-nanos1* and *Sp-nanos2*. Prime panels to the right of A–D are 3X zoom regions indicated by dashed boxes. DNA is labeled with Hoechst (blue). (E) In gastrula, Sp-Nanos1 and 2 protein is detected by immunoblot in uninjected embryos, but not in *Sp-nanos1/2* MASO-injected embryos. YP30 is used as a loading control and 200 embryos are loaded per lane.

lino oligonucleotide (MASO) knock down strategy. The immediate sequences upstream of the start codon in the 5′UTR of both *Sp-nanos1* and *Sp-nanos2* are identical, thus allowing us to design one morpholino to simultaneously knockdown both Sp-Nanos1 and Sp-Nanos2 protein expression. This morpholino will be referred to as *Sp-nanos1/2* MASO. *Sp-nanos1/2* MASO was injected into newly fertilized zygotes, which were subsequently cultured to the gastrula stage and analyzed for Sp-Nanos1 and 2 protein expression. Sp-Nanos1 and 2 proteins were no longer detected at gastrula stages by immunoblot analysis or by immunofluorescence in *Sp-nanos1/2* MASO-injected embryos as compared to uninjected controls (Fig. 3). Therefore, this morpholino effectively knocks down Sp-Nanos1 and 2 proteins.

To examine the effect of *Sp-nanos1 and 2* knockdown on small micromere development during embryogenesis we tested its effect on the expression of *Sp-vasa*, a well-characterized small micromere enriched gene (Voronina et al., 2008). *Sp-vasa* mRNA levels do not significantly change over the first 7 days of development after *Sp-nanos1* and *2* knockdown as indicated by real-time quantitative PCR (QPCR) (data not shown). As shown by WMISH, the *Sp-vasa* mRNA accumulation pattern is not disrupted by *Sp-nanos1* and *2* knockdown; *Sp-vasa* mRNA is detected at the vegetal plate of the blastula, in the small micromeres of the gastrula, and in both coelomic pouches of the pluteus in both *Sp-nanos1* and *2* knockdown embryos and controls (Figs. 4A–H). By contrast, when *Sp-nanos1* and *2* are knocked down, Sp-Vasa protein accumulation in the small micromere descendants is reduced at the gastrula stage as compared to mock-injected controls (Figs. 4K, L; Voronina et al., 2008).

Sp-nanos1 and Sp-nanos2 are required to maintain a wildtype number of small micromere descendants in the gastrula

Four small micromeres arise from an asymmetric division of the micromeres as the embryo develops from the 16-cell to 32-cell stage. Subsequently, the small micromeres divide once when in the vegetal plate of the blastula and then remain quiescent for the rest of embryogenesis. Therefore, 8 small micromere descendants travel at the tip of the archenteron and then are incorporated into the coelomic pouches of the pluteus. However, by WMISH, *Sp-nanos1* and *2*

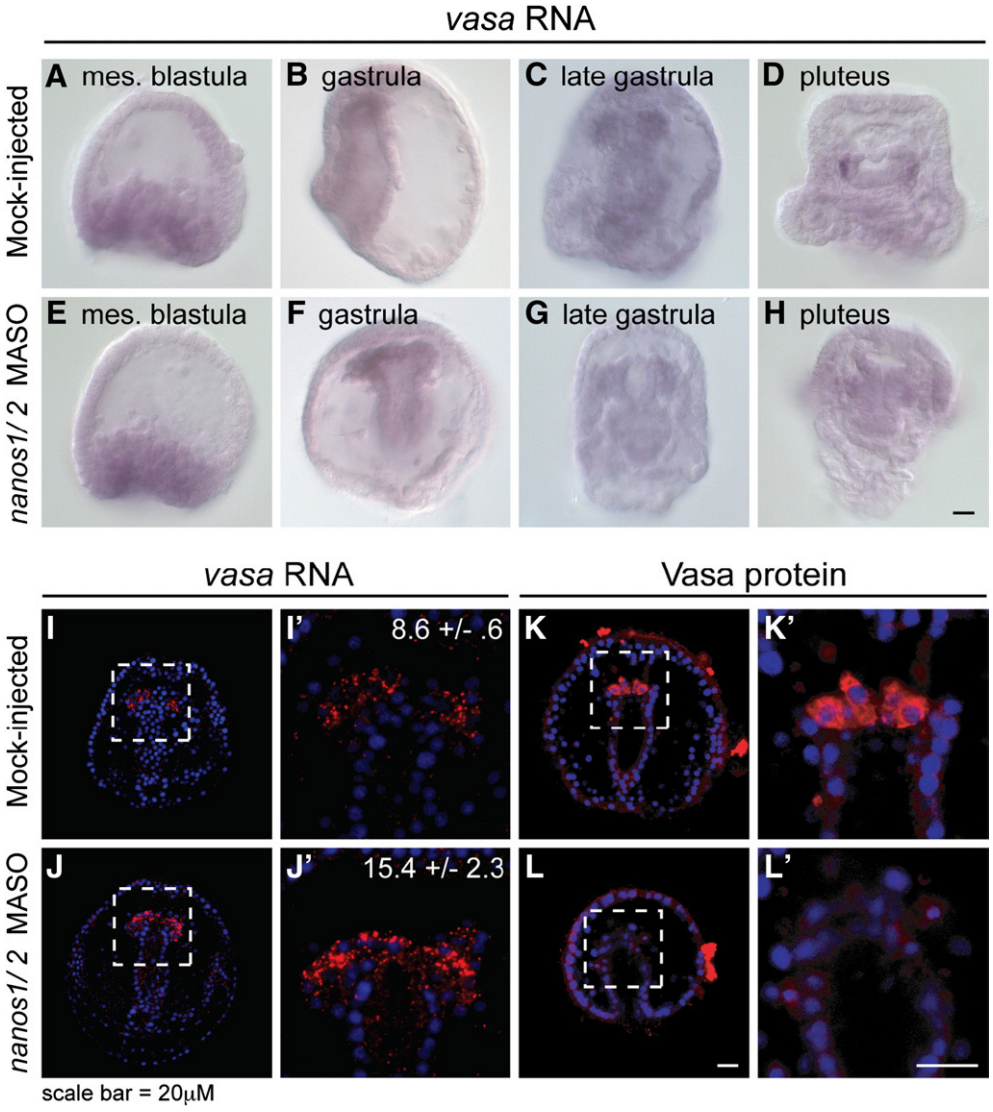

Fig. 4. *Sp-nanos1* and *2* knockdown gastrula have twice the number of *Sp-vasa* RNA-positive cells at the tip of the archenteron in the gastrula, but do not accumulate Sp-Vasa protein. (A–H) Depletion of Sp-Nanos1 and 2 protein has no effect on the accumulation pattern of *Sp-vasa* mRNA as shown by WMISH. Larva were collected at approximately 72 h. (I, J) *Sp-vasa* RNA FISH (red) and Hoechst labeling (blue) was performed to count the number of small micromere descendants at the tip of the archenteron. For each embryo analyzed, the number of *Sp-vasa*-positive cells was counted from confocal z-stacks. (I) Control gastrulae averaged 8.6 *Sp-vasa*-positive cells at the tip of the archenteron. (J) *Sp-nanos1* and *2* knockdown gastrulae averaged 15.4 *Sp-vasa*-positive cells at the tip of the archenteron. (K, L) As compared to mock-injected embryos, Sp-Vasa protein accumulation is reduced in the small micromere descendants of *Sp-nanos1* and *2* knockdown gastrula. Prime panels are zoomed-in regions indicated by dashed boxes in corresponding non-prime panels.

knockdown gastrulae appear to have an increased number of cells at the tip of the archenteron that accumulate *Sp-vasa* and *Sp-nanos1* and *2* transcripts. (Figs. 4F, 8G). To quantitate their number, fluorescent *in situ* hybridization (FISH) was used in combination with Hoechst labeling to count the number of *Sp-vasa* RNA-positive cells (Figs. 4I, J). *Sp-nanos1* and *2* knockdown gastrulae contain approximately twice the number of *Sp-vasa* RNA-positive cells at the tip of the archenteron. This may indicate that neighboring cells have acquired *Sp-vasa* mRNA expression. However, given that the number of *Sp-vasa* mRNA-positive cells is approximately double, it is more likely that the small micromere descendants have undergone one extra cell division. Therefore, *Sp-nanos1* and *2* may be required to maintain the mitotically quiescent state of the small micromeres during embryogenesis, an important feature of set-aside cells.

Sp-nanos1 and Sp-nanos2 are required for adult rudiment formation

Aside from the changes in the small micromere lineage described above, *Sp-nanos1* and *2* knockdown embryos proceed through embryogenesis normally, leading to formation of a pluteus larva, similar to mock-injected controls (Figs. 5A, D). However, when larvae that develop from *Sp-nanos1* and *2* knockdown embryos are fed and cultured, their coelomic pouches fail to grow and the rudiment does not form (Figs. 5E, F, J, O). With prolonged culture, *Sp-nanos1* and *2* knockdown larvae die after 4–6 weeks; these larvae are smaller than controls, but this lack of growth does not appear to be due to an inability to feed because the gut contracts and algae are present in the stomach. By contrast, larvae that develop from mock-injected embryos under the same culture conditions construct adult rudiments and can be induced to metamorphose (Figs. 5B, C, G, M, N).

Two-week-old control and *Sp-nanos1* and *2* knockdown larvae were assessed for Sp-Vasa protein accumulation by immunofluorescence (Figs. 5H, I, K, L). In control larvae Sp-Vasa protein is detected in the developing adult rudiment as well as the amniotic invagination (Figs. 5H, I). Of note here is that the amniotic invagination is of ectodermal origin, and thus the expression of Sp-Vasa protein in this region must be new (Pearse and Cameron, 1991). This is in contrast to the Vasa-positive cells in the developing rudiment, many of which are likely small micromere descendants. In larvae that develop from *Sp-nanos1* and *2* knockdown embryos, only a small number of Vasa-positive cells are detected in the poorly developing coelomic pouch and the amniotic invagination does not form (Figs. 5K, L).

To determine the relative contributions of *Sp-nanos1* and *Sp-nanos2* to coelomic pouch formation, two additional morpholinos

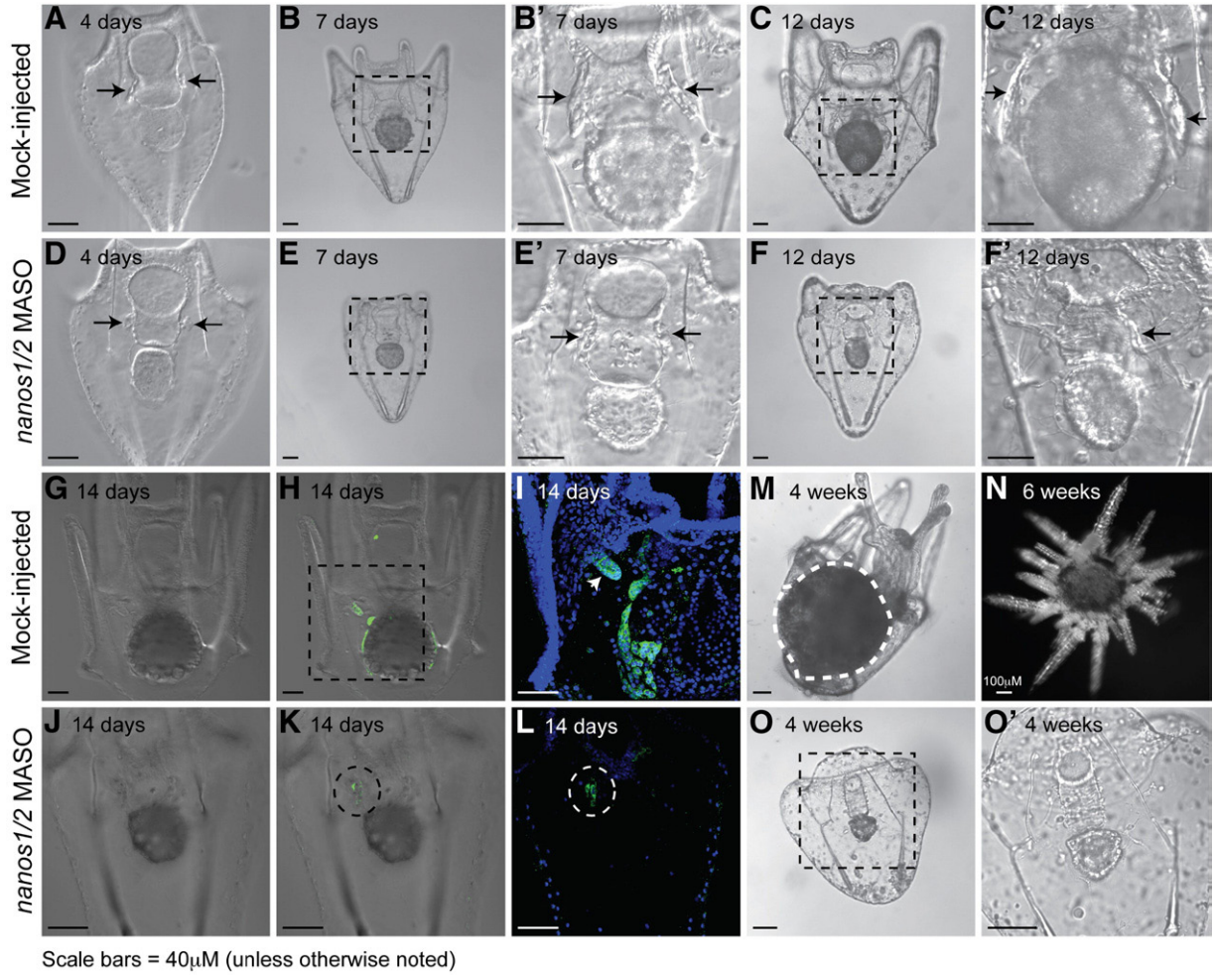

Fig. 5. *Sp-nanos1* and *Sp-nanos2* are required for larval pouch and rudiment development. Zygotes were injected with either red dextran alone (A–C, G–I, M, N) or with *Sp-nanos1* and *2* MASO (D–F, J–L, O) and cultured to the indicated larval stages. (A–H) As compared to mock-injected controls, the coelomic pouches of *Sp-nanos1* and *2* knockdown larvae fail to develop after 2 weeks of development. Arrows point to coelomic pouches. (G–I) Mock-injected and (J–L) *Sp-nanos1* and *2* knockdown larvae were immunolabeled with Sp-Vasa antibody (green) and counterstained with Hoechst (blue). (G–I) The developing coelomic pouches and amniotic invagination (arrowhead) of 2-week-old control embryos accumulate Sp-Vasa protein. (J) Only a small number of Sp-Vasa-positive cells (dashed circles in K and L) are detected in 2-week-old larvae cultured from *Sp-nanos1* and 2 knockdown embryos. (M, N) After 4 weeks of development, adult rudiments (white dotted circle) form normally in mock-injected larvae, which can be induced to metamorphose. (O) Four weeks after zygotic injection of *Sp-nanos1/2* MASO, larvae have not grown and adult rudiments have not formed; larvae die between 4 and 6 weeks after injection. Panels I and L are projections of confocal Z-stacks. Prime panels are zoomed-in regions indicated by dashed boxes in corresponding non-prime panels.

were designed to specifically target each *nanos* homolog. This was possible because approximately 40 bases upstream of the starting methionine the 5′UTR sequences of *Sp-nanos1* and *Sp-nanos2* diverge. *Sp-nanos1* knockdown larvae lacked significant coelomic pouches at 1 week and did not recover them, similar to *Sp-nanos1* and *2* knockdown larvae (Fig. 6B). *Sp-nanos2* knockdown larvae initially displayed a delay in coelomic pouch growth, but recovered and developed a normal adult rudiment (Fig. 6C, data not shown). When *Sp-nanos1* and *Sp-nanos2* are knocked down together by co-injection of both specific morpholinos, the phenotype is more severe than *Sp-nanos1* knockdown alone (Fig. 6D). Therefore, both *Sp-nanos1* and *Sp-nanos2* play an important role in coelomic pouch development, but *Sp-nanos1* is relatively more important as larvae cannot form an adult rudiment when this gene is knocked down by itself.

To test if the aberrant phenotype induced by the *Sp-nanos1* morpholino is due entirely to the loss of *Sp-nanos1* expression, a rescue experiment was performed (Figs. 6E, F). When *Sp-nanos1* mRNA with a morpholino-insensitive 5′UTR was co-injected with the *Sp-nanos1* morpholino, larvae were able to recover both their proper shape and size, and coelomic pouches developed normally (Fig. 6F). Furthermore, the Vasa-positive amniotic invagination was observed, which is not of coelomic pouch origin (Fig. 6F'). Thus, the dramatic larval phenotypes observed in *Sp-nanos1* morpholino-injected larvae are due entirely to the loss of *Sp-nanos1* expression.

Sp-nanos1 and Sp-nanos2 are required to maintain the larval fate of the small micromere lineage

We next tested the effect of *Sp-nanos1* and *2* knockdown specifically in the micromere lineage of an otherwise wild type embryo. To accomplish this, micromeres were transplanted from an *Sp-nanos1* and *2* knockdown (*Sp-nanos1/2* MASO plus red dextran) or mock-injected (red dextran only) 16-cell embryo to an uninjected recipient 16-cell embryo whose micromeres were previously removed (Fig. 7A). This experiment allows us to follow the fate of *Sp-nanos1* and *2* knockdown small micromeres during development. Furthermore, it tests if the requirement for *Sp-nanos1* and *2* in coelomic pouch development is specific to the micromere lineage. This lineage gives rise both to the small micromere lineage and to the large micromere lineage, which contributes solely to the larval skeleton.

After each transplant experiment, in both *Sp-nanos1* and *2* knockdown embryos and controls, labeled small micromere descendants were observed at the tip of the archenteron (data not shown). Furthermore in 5/5 control transplant embryos, labeled cells were observed in both coelomic pouches of an early pluteus (Figs. 7B, C). However, in 7/8 *Sp-nanos1* and *2* knockdown transplants, labeled cells were not observed in coelomic pouches indicating that the small micromere descendants were not incorporated there (Figs. 7E, F). In the one case where small micromeres were observed in the coelomic pouches, the intensity of the fluorescence was notably lower likely indicating a lower amount of morpholino injected in the donor embryo. The presence of red, large micromere-derived, skeletal cells in each case confirms a successful micromere transplant (Figs. 7D, G).

Larvae that develop from embryos with transplanted *Sp-nanos1* and *2* knockdown micromeres are able to develop adult rudiments to varying degrees (Figs. 7H–M). This is in contrast to larvae that develop from *Sp-nanos*1/2 MASO-injected zygotes, which are not able to make an adult rudiment (Fig. 5O). This result may indicate that in a wildtype embryo *Sp-nanos1* and/or *Sp-nanos2* are required outside of the small micromere lineage for proper coelomic pouch formation and adult rudiment development. Neither gene product is detected by WMISH outside of this lineage in wildtype embryos or larvae through 1 week of development, but this does not rule out low levels of expression in additional cell lineages. Alternatively, this result may indicate that when the descendants of *Sp-nanos1* and *2* knockdown small micromeres are not incorporated into the coelomic pouches, new *Sp-nanos1* and/or *2* expression in non-small micromere descendants rescues the adult rudiment. This rescue would not be possible when the *Sp-nanos1/2* MASO is ubiquitously present because newly transcribed *Sp-nanos1* and *2* mRNA would not be translated. In support of this latter hypothesis, *Sp-nanos1* and *2* knockdown embryos exhibit a 2-fold increase in *Sp-nanos1* and *2* mRNA accumulation, suggesting that the embryo compensates for the loss of Sp-Nanos1 and 2 protein by upregulating *Sp-nanos1* and/or *2* transcription (Fig. 8A). Furthermore, after *Sp-nanos1* and *2* knockdown, *Sp-nanos1* and *2* mRNA is detectable in the left coelomic pouch several days into larval

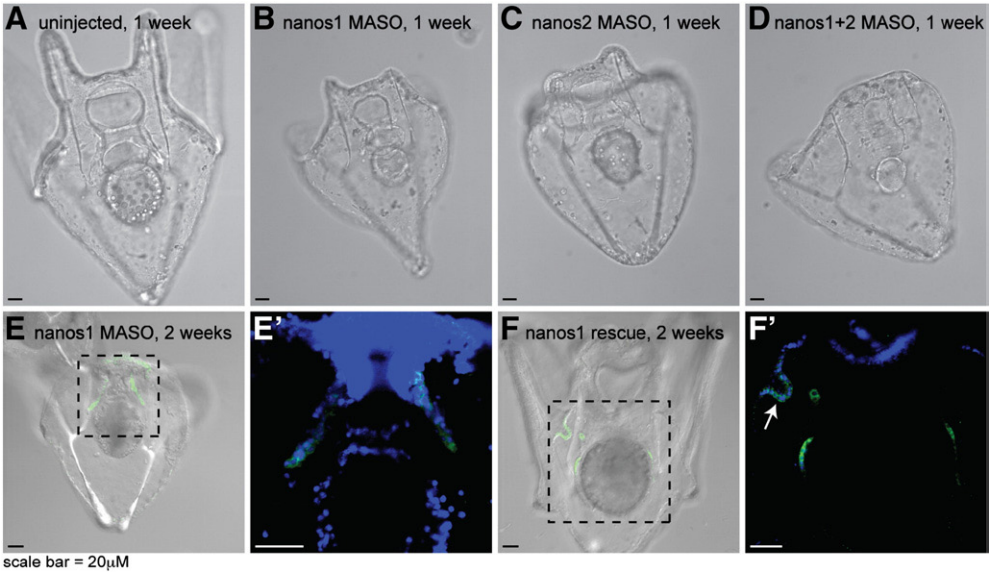

Fig. 6. *Sp-nanos1* and *Sp-nanos2* are independently required for proper larval coelomic pouch formation. Two additional morpholinos were designed to specifically target *Sp-nanos1* and *Sp-nanos2* further upstream of the ORF where the 5′ UTR diverges between these two homologs. (A) After 1 week of development, coelomic pouches are clearly visible in uninjected larvae. After zygotic injection of (B) *Sp-nanos1* MASO, (C) *Sp-nanos2* MASO, or (D) both morpholinos, coelomic pouch formation is delayed after 1 week of development. Larval defects caused by *Sp-nanos1* MASO (E) are corrected by simultaneous injection *of Sp-nanos1* MASO and *Sp-nanos1* mRNA (F). (E', F') Larvae are immunolabeled with Sp-Vasa antibody (green) and counterstained with Hoechst (blue). Arrow points to the amniotic invagination in the rescued larva. Prime panels are zoomed-in regions indicated by dashed boxes in corresponding non-prime panels.

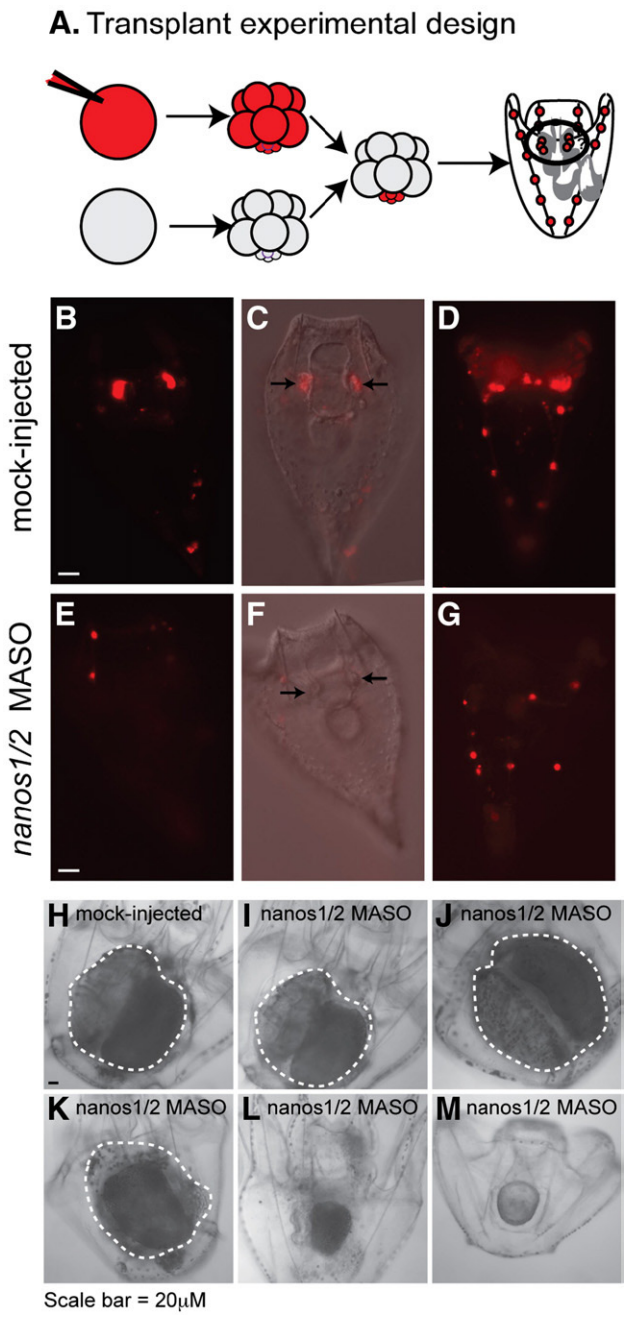

Fig. 7. *Sp-nanos1 and 2* knockdown small micromeres are not incorporated into the coelomic pouches, but adult rudiments can form. (A) Zygotes were injected with *Sp-nanos1/2* MASO plus red dextran or red dextran alone and then cultured to the 16-cell stage. The micromeres were removed from injected embryos and transplanted onto uninjected micromere-less 16-cell recipient embryos. Embryos were cultured to the pluteus stage (4 days), and then analyzed for the location of red dextran-positive cells. (B, C) In plutei resulting from control transplants, red dextran-positive small micromeres were always incorporated into the coelomic pouches (5/5). (E, F) *Sp-nanos1/2* MASO-injected small micromeres are not incorporated into the coelomic pouches; in 8 transplants, red dextran-positive cells were found in the coelomic pouches once. (D, G) In a different focal plane, red dextran-positive skeletal cells can be observed in both control and experimental plutei, thus demonstrating successful micromere transplants in each case. (C, F) Red fluorescence images were overlaid on the corresponding DIC images; arrows indicate coelomic pouches. (H) Control transplant larvae develop an adult rudiment by 5 weeks. (I–M) Larvae that developed from *Sp-nanos1/2* MASO transplants (e.g. panel E) were able to form adult rudiments in the same time frame as controls, but not in all cases (e.g. L and M). Adult rudiments are circled with a white dashed line.

development by WMISH (Fig. 8F–I). By contrast, in control larvae, *Sp-nanos1* and *2* mRNA is no longer detected by WMISH shortly after pluteus formation (Figs. 8B–E). Given that the *Sp-nanos1* and *2* knockdown small micromeres are not incorporated into the coelomic pouches (see Fig. 7), this result suggests that an alternative cell population is accumulating *Sp-nanos1* and/or *2* mRNA in the coelomic pouch of *Sp-nanos1* and *2* knockdown larvae. Furthermore, this new population of *Sp-nanos1* and/or *2*-positive cells may be responsible for the recovery of the adult rudiment observed in our transplant experiments (see Fig. 7).

Discussion

Nanos is required to maintain the fate of the small micromere lineage

Sp-nanos1 and *2* are required for the incorporation of the small micromere descendants into the larval coelomic pouches and are therefore critical to maintain small micromere fate. Furthermore, in the absence of *Sp-nanos1* and *2*, coelomic pouches do not develop and the adult rudiment does not form, thus the functions of these genes are required for juvenile development (Fig. 9). Given that *Sp-nanos1* and *2* are specifically expressed in the small micromere lineage, this suggests that these cells are multipotent and give rise to multiple juvenile tissues. Alternatively, the small micromere descendants could have a critical signaling role in directing proliferation and fate determination in other cells that contribute to coelomic pouch and adult rudiment formation. These two possibilities are not mutually exclusive and currently we cannot distinguish between their relative contributions to adult rudiment development. The small micromere descendants proliferate rapidly upon their arrival at the coelomic pouch, which supports the hypothesis that these cells contribute substantially to the adult rudiment, and are therefore multipotent (Tanaka and Dan, 1990). The complete lack of adult rudiment structures in the *Sp-nanos1* and *2* knockdowns also implies that other cells that contribute to juvenile development require the presence of the small micromere lineage to adopt their fates. For example, the cells of the amniotic invagination do not invaginate in *Sp-nanos1* and *2* knockdown larvae. Thus, the small micromere lineage may contribute to adult rudiment development both by contributing directly to the tissues and in an instructive manner.

The sea urchin larva can recover small micromere fates

Although the sea urchin embryo is patterned very early by maternal inputs and zygotic gene expression, some of the cells retain plasticity, thus allowing for remarkable regulative capacity. For example, the large micromere descendants give rise to the primary mesenchyme cells (PMCs), which ingress into the blastocoel before gastrulation and eventually give rise to the entire larval skeleton. However, if the PMCs are surgically removed from the early gastrula then a population of non-skeletal mesenchyme cells transfate into skeletal mesenchyme cells and a larval skeleton is built (Ettensohn and McClay, 1988; Ettensohn et al., 2007). If the micromeres are removed at the 16-cell stage then both the large and small micromere lineages are lost. However, the resulting larvae have a skeleton and develop an adult rudiment that produces normal, fertile adults (Ransick et al., 1996). Given the significant contribution of the small micromeres to the coelomic pouches, this result suggests that micromere-deleted embryos successfully recover multipotent cells for adult rudiment formation.

Recent work demonstrated that the regulation of *Sp-vasa* expression might play an important role in the recovery of multipotent small micromere fates (Voronina et al., 2008). When the Vasa-positive micromeres are removed, Vasa protein expression is upregulated in the entire embryo, followed by a restriction to a subset of cells, which

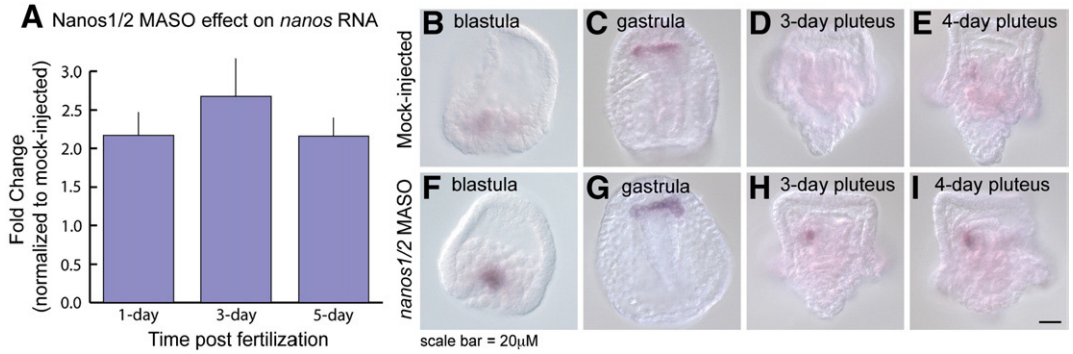

Fig. 8. Sp-Nanos1 and 2 knockdown leads to an increase in *Sp-nanos1* and *2* mRNA levels and sustained accumulation of *Sp-nanos1* and *2* mRNA in the left coelomic pouch of early plutei. Zygotes were injected with either *Sp-nanos1/2* MASO or red dextran alone and then collected at the indicated time points for WMISH and QPCR. (A) As indicated by QPCR, *Sp-Nanos 1* and *2* knockdown causes a 2-fold increase in the level of *Sp-nanos1* and *2* mRNA. (B–I) In contrast to the mock-injected controls, *Sp-nanos1 and 2* mRNA is detected in the coelomic pouches of *Sp-nanos1* and *2* knockdown larvae.

may then take on the fate of the former small micromere lineage (Voronina et al., 2008). Here we demonstrate that *Sp-nanos1* and *2* knockdown embryos develop into larvae that cannot produce an adult rudiment. Interestingly, when *Sp-nanos1* and *2* knockdown is restricted to the micromere lineage, the resulting larvae are capable of producing an adult rudiment, despite the fact that the small micromeres are not incorporated into the coelomic pouches. This result implies that the embryo is able to recover the lost population of multipotent cells early in larval development. New expression of *Sp-nanos1* and/or *2* must be required for the specification of new multipotent cells because adult rudiments cannot form when the *Sp-nanos1/2* MASO is ubiquitously present. In *Sp-nanos1* and *2* knockdown embryos, accumulation of *Sp-nanos1* and *2* RNA is increased and persists in the coelomic pouch further into larval development. Given that macromere descendants are the only other lineage to populate the coelomic pouches, these cells may take on small micromere fates when the small micromere descendants are lost.

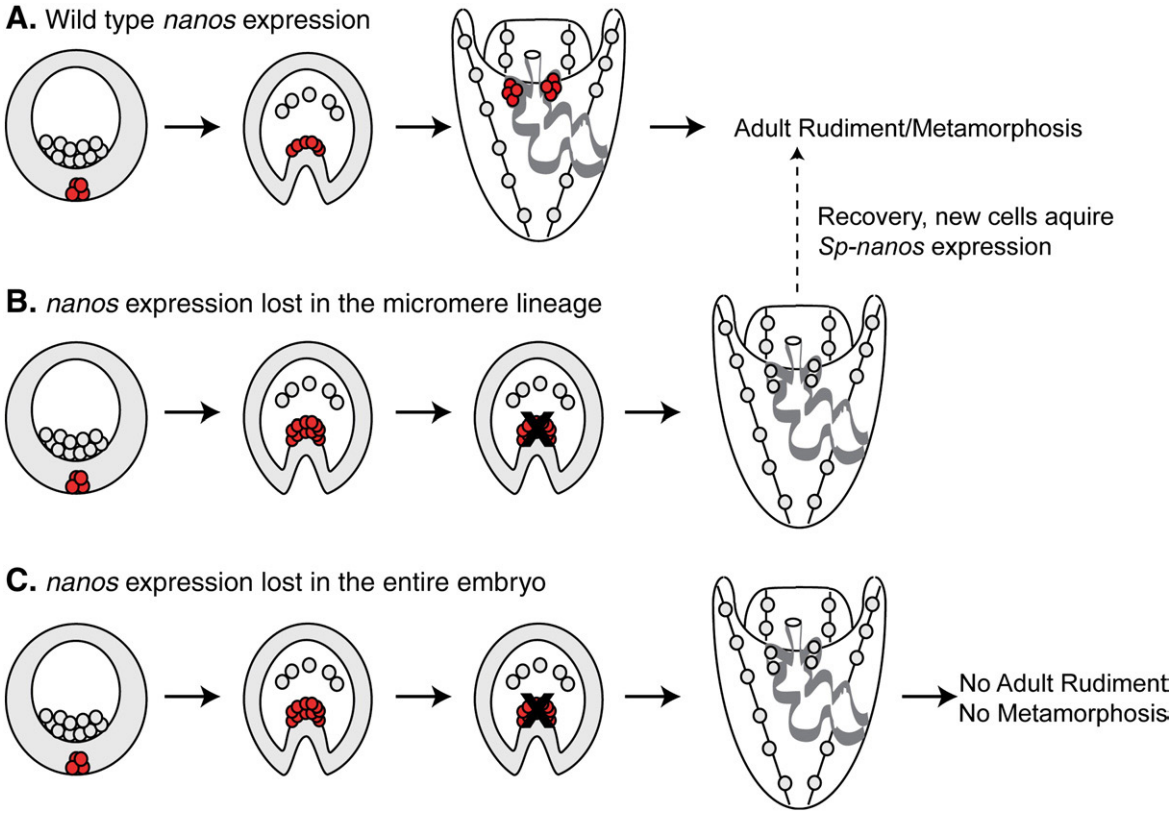

Fig. 9. *Sp-nanos1* and *Sp-nanos*2 are required to maintain small micromere quiescence, for incorporation of the small micromeres into the coelomic pouches, and for adult rudiment formation. (A) During normal development, the four small micromeres (red) are present in the vegetal plate where they divide once before traveling through the blastocoel at the tip of the archenteron during gastrulation. The small micromere descendants are incorporated into the coelomic pouches where they contribute to adult rudiment formation. (B) When *Sp-nanos1* and *2* knockdown is restricted to the micromere lineage in transplant experiments, the small micromere descendants are not incorporated into the pouches, but the rudiment is able to form. We hypothesize that this recovery is due to new *Sp-nanos1* and/or *Sp-nanos2* expression in macromere descendants that also populate the coelomic pouches. (C) In *Sp-nanos1* and *2* knockdown embryos, twice the number of small micromere descendants (identified by *Sp-vasa* mRNA accumulation) is observed at the tip of the archenteron in the gastrula. Subsequently, the small micromere descendants are not incorporated into the coelomic pouches, the adult rudiment does not form, and larvae do not survive.

Nanos has a conserved function in maintaining the fate of PGCs and multipotent cells

Nanos is required to maintain germline fate throughout the *Drosophila* life cycle and appears to have a similar function in maintaining germline fate in other organisms. In *C. elegans* embryos and larvae, *nanos* is required to maintain repressive chromatin marks and cell cycle arrest (Subramaniam and Seydoux, 1999; Schaner et al., 2003). In the mouse, *nanos3*$^{-/-}$ PGCs undergo apoptosis (Tsuda et al., 2003; Suzuki et al., 2008). In adult germlines *nanos* is required to maintain oocyte production in zebrafish and spermatogonia populations in mice (Draper et al., 2007; Lolicato et al., 2008). Therefore, *nanos* has a conserved function in preserving animal germlines by maintaining a quiescent state.

The function of *nanos* in the small micromeres appears to be analogous to its conserved germline functions. Small micromere descendants in *Sp-nanos1* and *2* knockdown embryos may undergo an extra division and are not incorporated into the coelomic pouches. We do not know what happens to *Sp-nanos1* and *2* knockdown small micromeres, but two possibilities exist. First, they may undergo apoptosis, similar to *nanos*$^{-/-}$ pole cells in *Drosophila* and *nanos3*$^{-/-}$ PGCs in mice (Tsuda et al., 2003; Hayashi et al., 2004; Sato et al., 2007; Suzuki et al., 2008). Alternatively, *nanos*-depleted small micromere descendants may take on differentiated cell fates and thus become incorporated into other larval structures. This outcome would be analogous to *Drosophila* pole cells taking on somatic cell fates when the apoptosis pathway is suppressed (Hayashi et al., 2004). However, no evidence of small micromere incorporation into alternative larval structures was detected in our transplant experiments, thus we favor the hypothesis that *nanos*-depleted small micromeres undergo apoptosis.

A conserved molecular program in multipotent cells?

The small micromere lineage specifically expresses *vasa*, *nanos*, and *piwi*, all of which have conserved roles in germline determination and maintenance, yet the small micromeres do not appear to give rise exclusively to germ cells (Juliano et al., 2006). We propose that the sea urchin uses a two-step germline determination mechanism. The first step is the formation of an embryonic multipotent precursor under the control of a conserved molecular program, which includes specific expression of *nanos*, *vasa*, and, *piwi*. In the second step of this mechanism the multipotent precursors give rise to both somatic cells and to germ cells later in development. In the sea urchin, this likely occurs as the adult rudiment forms during larval development. This mechanism is in contrast to animals that only exhibit specific expression of *vasa*, *nanos*, and *piwi* in cells fated to be exclusively germline, which we refer to here as one-step germline determination. The two-step germline determination mechanism was also proposed for *P. dumerilii*, a lophotrochozoan that segregates its germline late in larval development from a multipotent precursor established during embryogenesis. This lineage of multipotent cells is termed the mesodermal growth zone (MPGZ) and like the small micromere lineage of the sea urchin, cells of the MPGZ specifically express *vasa*, *nanos*, and *piwi* (Rebscher et al., 2007). *Vasa* and *nanos* also are expressed specifically in the 4d lineage of *Ilyanassa*, another lophotrochozoan and loss of *nanos* leads to significant loss of adult structures derived from this lineage (Rabinowitz et al., 2008; Swartz et al., 2008). This same program also may operate in the multipotent I-cells of the adult *Hydra*, a cnidarian. *Vasa* and *nanos* are specifically expressed in *Hydra* I-cells, which give rise both to somatic cells and to germ cells (Mochizuki et al., 2000, 2001). Conservation of the gene expression profiles and of *nanos* function in PGCs and various multipotent cell lineages suggests the presence of a conserved molecular program shared in these cell types. What is the evolutionary relationship between cells that contain this program among metazoans? We propose the following two mutually exclusive hypotheses to explain how the small micromeres obtained this program:

(1) *Two-step germline determination is ancestral* (Fig. 10A): the echinoderm embryo uses an ancient two-step germline specification process in which the PGCs are segregated from multipotent precursors late in development. In this scenario, the lophotrochozoans and the echinoderms use the same ancestral 2-step germline determination mechanism and their multi-

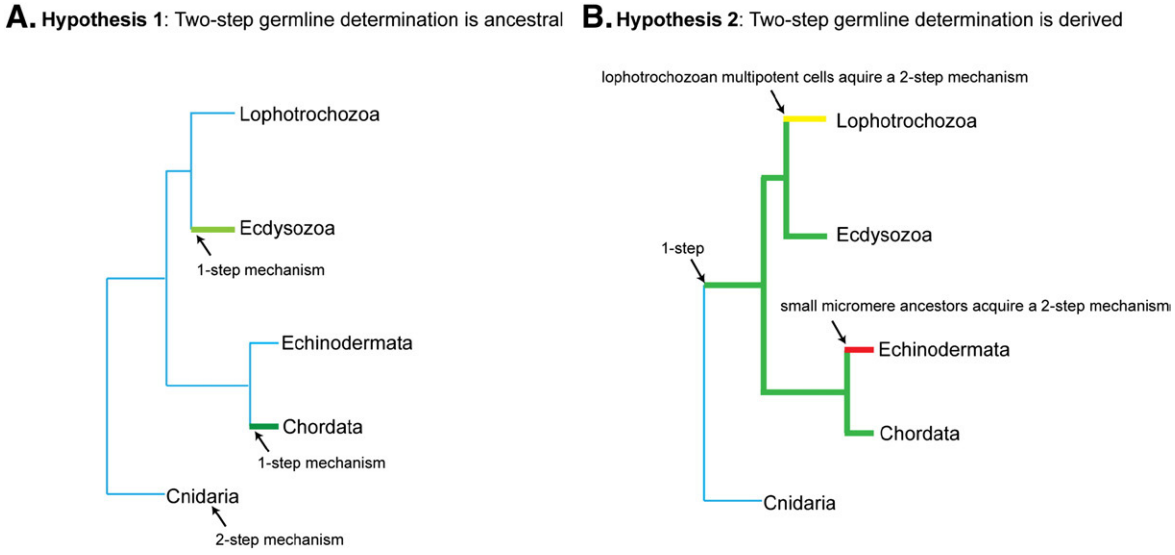

Fig. 10. Two mutually exclusive hypotheses to explain how the small micromere lineage obtained its multipotency molecular program. (A) Hypothesis 1: two-step germline determination is ancient. The direct-developing ancestor used an ancestral 2-step germline determination mechanism similar to modern cnidarians (blue), which was retained by the maximally indirect-developing echinoderms. The lophotrochozoans and echinoderms use the same ancient 2-step mechanism and obtained their multipotency molecular program from a common origin. In this scenario the acquisition of 1-step PGC specification in some chordates and ecdysozoans must have occurred independently (green). (B) Hypothesis 2: two-step germline determination is derived. In this scenario the last common bilatarian ancestor used 1-step PGC specification (green), which is still used by some chordates and ecdysozoans. During the transition from direct to maximally indirect development, the ancestor of the small micromere lineage co-opted the primordial germ cell (PGC) molecular program from the adult (red). A similar scenario must also have occurred in the lophotrochozoans (yellow).

potent precursors have obtained their molecular program from a common origin. This ancestral program, which includes *vasa*, *nanos*, and *piwi*, may also be used by cnidarians to specify and maintain multipotent I-cells. This model argues that the acquisition of a 1-step PGC specification in some chordates and ecdysozoans (e.g. mice and *Drosophila*) occurred independently.

(2) *Two-step germline determination is derived* (Fig. 10B): in this model the bilatarian ancestor used a 1-step PGC specification, which is still used by some chordates and ecdysozoans. These organisms used *vasa*, *nanos*, and *piwi* in cells that are destined to become exclusively germline. In this scenario, the lophotrochozoans and echinoderms independently acquired a two-step germline determination mechanism.

Maximal indirect development is prevalent in both the lophotrochozoans and in echinoderms, although substantial evidence suggests that these branches independently acquired this form of development (Raff, 2008). Therefore, a correlative link exists between maximal indirect development and the two-step germline determination mechanism. If the two-step germline determination is ancestral (Fig. 10A) then perhaps it was the retention of this mechanism that facilitated the independent acquisition of maximal indirect development. In such a case, pre-existing multipotent precursors could easily be set aside for use in the adult, thus protecting the germline during the transition. Furthermore, the acquisition of maximal indirect development may have locked many echinoderms and lophotrochozoans into an ancestral two-step germline determination mechanism. By contrast, if two-step germline determination is derived (Fig. 10B), then it may have independently evolved in these two groups with maximal indirect development. It has been hypothesized that the larvae of maximal indirect developers co-opted GRNs from the adult for use in building its larval structures (Sly et al., 2003). For example, the GRN used to build the sea urchin larval skeleton was likely co-opted from the adult skeletogenic GRN (Gao and Davidson, 2008). Therefore, if two-step germline determination is derived, it is possible that the small micromere lineage co-opted its molecular program from adult PGCs.

These models are based on data from a limited number of animal species. To discern the evolutionary origins of the small micromere molecular program it is critical to decorate the tree with data from a wide variety of organisms. However, based on this study and those reported in *Hydra*, planarians, *Ilyanassa*, and *P. dumerilii* it is clear that genes traditionally classified as "germline genes" have a broader role in maintaining multipotency (Shibata et al., 1999; Mochizuki et al., 2000, 2001; Reddien et al., 2005; Salvetti et al., 2005; Guo et al., 2006; Juliano et al., 2006; Rebscher et al., 2007; Palakodeti et al., 2008; Rabinowitz et al., 2008; Swartz et al., 2008; Voronina et al., 2008). Specification and maintenance of potency in all of the cell types that express genes such as *vasa*, *nanos*, and *piwi* likely share a common underlying mechanism of regulatory control. Thus, comparing these mechanisms in diverse animals that use varied developmental strategies will allow us to uncover the critical and ancestral portions of this program.

Acknowledgments

We thank all current and past members of PRIMO for helpful discussions. Specifically we thank Zak Swartz and Adrian Reich for help in editing this manuscript. We thank two anonymous reviewers for helpful and critical feedback on this manuscript. This work was supported by grants from the NIH and the NSF.

Appendix A. Supplementary data

Supplementary data associated with this article can be found, in the online version, at doi:10.1016/j.ydbio.2009.10.030.

References

Altschul, S.F., Gish, W., Miller, W., Myers, E.W., Lipman, D.J., 1990. Basic local alignment search tool. J. Mol. Biol. 215 (3), 403–410.
Asaoka-Taguchi, M., Yamada, M., Nakamura, A., Hanyu, K., Kobayashi, S., 1999. Maternal Pumilio acts together with Nanos in germline development in Drosophila embryos. Nat. Cell Biol. 1 (7), 431–437.
Cameron, R.A., Fraser, S.E., Britten, R.J., Davidson, E.H., 1991. Macromere cell fates during sea urchin development. Development 113 (4), 1085–1091.
Cheers, M.S., Ettensohn, C.A., 2004. Rapid microinjection of fertilized eggs. In: Ettensohn, C.A., Wessel, G., Wray, G. (Eds.), Methods in Cell Biology: Development of Sea Urchins, Ascidians, and Other Invertebrate Deuterostomes: Experimental Approaches. Elsevier, pp. 287–310.
Deshpande, G., Calhoun, G., Yanowitz, J.L., Schedl, P.D., 1999. Novel functions of nanos in downregulating mitosis and transcription during the development of the Drosophila germline. Cell 99 (3), 271–281.
Draper, B.W., McCallum, C.M., Moens, C.B., 2007. nanos1 is required to maintain oocyte production in adult zebrafish. Dev. Biol. 305 (2), 589–598.
Ettensohn, C.A., McClay, D.R., 1988. Cell lineage conversion in the sea urchin embryo. Dev. Biol. 125 (2), 396–409.
Ettensohn, C.A., Kitazawa, C., Cheers, M.S., Leonard, J.D., Sharma, T., 2007. Gene regulatory networks and developmental plasticity in the early sea urchin embryo: alternative deployment of the skeletogenic gene regulatory network. Development 134 (17), 3077–3087.
Gao, F., Davidson, E.H., 2008. Transfer of a large gene regulatory apparatus to a new developmental address in echinoid evolution. Proc. Natl. Acad. Sci. 105 (16), 6091.
Guo, T., Peters, A.H., Newmark, P.A., 2006. A Bruno-like gene is required for stem cell maintenance in planarians. Dev. Cell 11 (2), 159–169.
Hayashi, Y., Hayashi, M., Kobayashi, S., 2004. Nanos suppresses somatic cell fate in Drosophila germ line. Proc. Natl. Acad. Sci. U. S. A. 101 (28), 10338–10342.
Juliano, C.E., Voronina, E., Stack, C., Aldrich, M., Cameron, A.R., Wessel, G.M., 2006. Germ line determinants are not localized early in sea urchin development, but do accumulate in the small micromere lineage. Dev. Biol. 300 (1), 406–415.
Kadyrova, L.Y., Habara, Y., Lee, T.H., Wharton, R.P., 2007. Translational control of maternal Cyclin B mRNA by Nanos in the Drosophila germline. Development 134 (8), 1519–1527.
Kobayashi, S., Yamada, M., Asaoka, M., Kitamura, T., 1996. Essential role of the posterior morphogen nanos for germline development in Drosophila. Nature 380 (6576), 708–711.
Koprunner, M., Thisse, C., Thisse, B., Raz, E., 2001. A zebrafish nanos-related gene is essential for the development of primordial germ cells. Genes Dev. 15 (21), 2877–2885.
Lolicato, F., Marino, R., Paronetto, M.P., Pellegrini, M., Dolci, S., Geremia, R., Grimaldi, P., 2008. Potential role of Nanos3 in maintaining the undifferentiated spermatogonia population. Dev. Biol. 313 (2), 725–738.
Minokawa, T., Rast, J.P., Arenas-Mena, C., Franco, C.B., Davidson, E.H., 2004. Expression patterns of four different regulatory genes that function during sea urchin development. Gene Expr. Patterns 4 (4), 449–456.
Mochizuki, K., Sano, H., Kobayashi, S., Nishimiya-Fujisawa, C., Fujisawa, T., 2000. Expression and evolutionary conservation of nanos-related genes in Hydra. Dev. Genes Evol. 210 (12), 591–602.
Mochizuki, K., Nishimiya-Fujisawa, C., Fujisawa, T., 2001. Universal occurrence of the vasa-related genes among metazoans and their germline expression in Hydra. Dev. Genes Evol. 211 (6), 299–308.
Nagahara, H., Vocero-Akbani, A.M., Snyder, E.L., Ho, A., Latham, D.G., Lissy, N.A., Becker-Hapak, M., Ezhevsky, S.A., Dowdy, S.F., 1998. Transduction of full-length TAT fusion proteins into mammalian cells: TAT-p27Kip1 induces cell migration. Nat. Med. 4 (12), 1449–1452.
Palakodeti, D., Smielewska, M., Lu, Y.C., Yeo, G.W., Graveley, B.R., 2008. The PIWI proteins SMEDWI-2 and SMEDWI-3 are required for stem cell function and piRNA expression in planarians. RNA 14 (6), 1174–1186.
Pearse, J.S., Cameron, A.R., 1991. Echinodermata: Echinoidea. In: Giese, A.C., Pearse, J.S., Pearse, V.B. (Eds.), Reproduction of Marine Invertebrates. Boxwood Press, Pacific Grove, CA, pp. 514–664.
Pehrson, J.R., Cohen, L.H., 1986. The fate of the small micromeres in sea urchin development. Dev. Biol. 113 (2), 522–526.
Peterson, K.J., Cameron, R.A., Davidson, E.H., 1997. Set-aside cells in maximal indirect development: evolutionary and developmental significance. BioEssays 19 (7), 623–631.
Pfister, D., De Mulder, K., Hartenstein, V., Kuales, G., Borgonie, G., Marx, F., Morris, J., Ladurner, P., 2008. Flatworm stem cells and the germ line: developmental and evolutionary implications of macvasa expression in *Macrostomum lignano*. Dev. Biol. 319 (1), 146–159.
Rabinowitz, J.S., Chan, X.Y., Kingsley, E.P., Duan, Y., Lambert, J.D., 2008. Nanos is required in somatic blast cell lineages in the posterior of a mollusk embryo. Curr. Biol. 18 (5), 331–336.
Raff, R.A., 2008. Origins of the other metazoan body plans: the evolution of larval forms. Philos. Trans. R. Soc. Lond., B Biol. Sci. 363 (1496), 1473–1479.
Ransick, A., Cameron, R.A., Davidson, E.H., 1996. Postembryonic segregation of the germ line in sea urchins in relation to indirect development. Proc. Natl. Acad. Sci. U. S. A. 93 (13), 6759–6763.
Rebscher, N., Zelada-Gonzalez, F., Banisch, T.U., Raible, F., Arendt, D., 2007. Vasa unveils a common origin of germ cells and of somatic stem cells from the posterior growth zone in the polychaete *Platynereis dumerilii*. Dev. Biol. 306 (2), 599–611.
Reddien, P.W., Oviedo, N.J., Jennings, J.R., Jenkin, J.C., Sanchez Alvarado, A., 2005. SMEDWI-2 is a PIWI-like protein that regulates planarian stem cells. Science 310 (5752), 1327–1330.

Render, J., 1997. Cell fate maps in the *Ilyanassa obsoleta* embryo beyond the third division. Dev. Biol. 189 (2), 301–310.
Salvetti, A., Rossi, L., Lena, A., Batistoni, R., Deri, P., Rainaldi, G., Locci, M.T., Evangelista, M., Gremigni, V., 2005. DjPum, a homologue of Drosophila Pumilio, is essential to planarian stem cell maintenance. Development 132 (8), 1863–1874.
Sato, K., Hayashi, Y., Ninomiya, Y., Shigenobu, S., Arita, K., Mukai, M., Kobayashi, S., 2007. Maternal Nanos represses hid/skl-dependent apoptosis to maintain the germ line in Drosophila embryos. Proc. Natl. Acad. Sci. U. S. A. 104 (18), 7455–7460.
Schaner, C.E., Deshpande, G., Schedl, P.D., Kelly, W.G., 2003. A conserved chromatin architecture marks and maintains the restricted germ cell lineage in worms and flies. Dev. Cell 5 (5), 747–757.
Seki, Y., Yamaji, M., Yabuta, Y., Sano, M., Shigeta, M., Matsui, Y., Saga, Y., Tachibana, M., Shinkai, Y., Saitou, M., 2007. Cellular dynamics associated with the genome-wide epigenetic reprogramming in migrating primordial germ cells in mice. Development 134 (14), 2627–2638.
Seydoux, G., Braun, R.E., 2006. Pathway to totipotency: lessons from germ cells. Cell 127 (5), 891–904.
Shibata, N., Umesono, Y., Orii, H., Sakurai, T., Watanabe, K., Agata, K., 1999. Expression of vasa(vas)-related genes in germline cells and totipotent somatic stem cells of planarians. Dev. Biol. 206 (1), 73–87.
Sly, B.J., Snoke, M.S., Raff, R.A., 2003. Who came first-larvae or adults? Origins of bilaterian metazoan larvae. Int. J. Dev. Biol. 47 (7/8), 623–632.
Su, T.T., Campbell, S.D., O'Farrell, P.H., 1998. The cell cycle program in germ cells of the Drosophila embryo. Dev. Biol. 196 (2), 160–170.
Subramaniam, K., Seydoux, G., 1999. nos-1 and nos-2, two genes related to Drosophila nanos, regulate primordial germ cell development and survival in *Caenorhabditis elegans*. Development 126 (21), 4861–4871.
Suzuki, H., Tsuda, M., Kiso, M., Saga, Y., 2008. Nanos3 maintains the germ cell lineage in the mouse by suppressing both Bax-dependent and -independent apoptotic pathways. Dev. Biol. 318 (1), 133–142.
Swartz, S.Z., Chan, X.Y., Lambert, J.D., 2008. Localization of Vasa mRNA during early cleavage of the snail Ilyanassa. Dev. Genes Evol. 218 (2), 107–113.
Swofford, D.L. 2002. PAUP*: Phylogenetic Analysis Using Parsimony (*and other methods). Version 4. In. Sinauer Associates, Sunderland, MA.
Tanaka, S., Dan, K., 1990. Study of the lineage and cell cycle of small micromeres in embryos of the sea urchin, *Hemicentrotus pulcherrimus*. Dev. Growth Differ. 32 (2), 145–156.
Tsuda, M., Sasaoka, Y., Kiso, M., Abe, K., Haraguchi, S., Kobayashi, S., Saga, Y., 2003. Conserved role of nanos proteins in germ cell development. Science 301 (5637), 1239–1241.
Voronina, E., Lopez, M., Juliano, C.E., Gustafson, E., Song, J.L., Extavour, C., George, S., Oliveri, P., McClay, D., Wessel, G., 2008. Vasa protein expression is restricted to the small micromeres of the sea urchin, but is inducible in other lineages early in development. Dev. Biol. 314 (2), 276–286.
Wessel, G.M., Zaydfudim, V., Hsu, Y.J., Laidlaw, M., Brooks, J.M., 2000. Direct molecular interaction of a conserved yolk granule protein in sea urchins. Dev. Growth Differ. 42 (5), 507–517.
Wong, J.L., Wessel, G.M., 2004. Major components of a sea urchin block to polyspermy are structurally and functionally conserved. Evol. Dev. 6 (3), 134–153.
Yajima, M., 2007. Evolutionary modification of mesenchyme cells in sand dollars in the transition from indirect to direct development. Evol. Dev. 9 (3), 257–266.